Suppression of Tumorigenicity of Human Hepatocellular Carcinoma Cells by Antisense Oligonucleotide MZF-1

Yi-Hsien Hsieh[1], Trang-Tiau Wu[2], Chih-Yang Huang[3], Yih-Shou Hsieh[1] and Jer-Yuh Liu[1]

[1]*Institute of Biochemistry and Biotechnology*
Chung-Shan Medical University
[2]*Department of Surgery, School of Medicine*
Chung Shan Medical University
and
[3]*Graduate Institute of Chinese Medical Science*
China Medical University
Taichung, Taiwan, R.O.C.

Abstract

Our previous studies have found that reducing expression of myeloid zinc finger-1 (MZF-1) inhibited protein kinase C alpha (PKCα) expression and decreased cell migration and invasion in human hepatocellular carcinoma (HCC). In this study, we further investigated the role of MZF-1 in tumorigenesis. The SK-Hep-1 HCC cells were transfected with the antisense oligonucleotide (ODN) of MZF-1. The pretreated cells was then detected the mRNA and protein levels by RT-PCR and western blotting, and the cell growth was assayed by MTT. Meanwhile, the pretreated-SK-Hep-1 HCC cells were implanted subcutaneously into nude mice to observe the tumor growth and calculated tumor inhibitory rate. The results showed that, at the dosage of 5 μM, the antisense ODN MZF-1 suppressed both MZF-1 and PKCα productions by SK-Hep-1 HCC cells after cationic liposome-mediated transfection, to 15% and 30% in control cultures of 0 μM dosage, respectively. The growth of SK-Hep-1 HCC cells was inhibited by the 2-5 μM doses of the antisense ODN MZF-1, whereas the control reagent, the sense ODN MZF-1, showed no effects. In BALB/nude mice, SK-Hep-1 HCC cells pretreated with the 5 μM antisense ODN MZF-1 formed tumors much smaller than the cells with sense ODN. The mean of inhibitory rate of tumor growth was 71.2 ± 8.6%, and the tumor formation time was prolonged from 14 days to 26 days. These findings suggested the usefulness of antisense ODN MZF-1 as a new reagent for cancer therapy.

Key Words: myeloid zinc finger-1, tumorigenesis, antisense oligonucleotide

Introduction

Zinc-finger family of proteins is one of the most common families of transcription factors in eukaryotic cells and has more than 3,000 members in the human genome. They are known to play a key role in regulating expression of genes important for cell growth, proliferation, differentiation and apoptosis (5, 13, 18). Owing to their multiple functions, some zinc-finger proteins are powerful regulators in the development of the tumour. For examples of zinc-finger proteins involved in tumorigenesis include those encoded by the genes of GLI, KS1, Evi9 and BCL11 subfamilies. However, the role of the remainders of the zinc-finger family in tumour development is not clear yet (7, 14). Therefore, investigation of additional zinc-finger proteins associated with tumorigenesis may provide insight into molecular mechanisms underlying tumorigenesis.

Myeloid zinc finger 1 (MZF-1) is a transcription factor of the Kruppel family proteins originally cloned from a cDNA library from a patient with chronic myeloid

Corresponding author: Dr. Jer-Yuh Liu, Institute of Biochemistry and Biotechnology, College of Medicine, Chung-Shan Medical University, Taichung 402, Taiwan. Tel: +886-4-24730022 ext. 11673, Fax: +886-4-23248195, E-mail: jyl@csmu.edu.tw
Received: March 11, 2006; Revised (Finally): June 8, 2006; Accepted: June 28, 2006.

leukemia (9). Human MZF-1 encodes a 485-amino acid protein that contains 13 zinc fingers divided into two groups, which can independently of bind the DNA each other (15). MZF-1 is preferentially expressed in myeloid leukemia cell lines and myeloid progenitor cells from normal marrow (16) and may regulate the expression of specific gene in a tissues-specific manner (17). MZF-1 expression is both necessary for hematopoietic cell differentiation (3) and is critical to the regulation of cell proliferation and apoptosis (10, 11, 19). However, the biological function of MZF-1 in HCC progression is still unknown.

Previously our studies found that reducing expression of MZF-1 would inhibit PKCα expression and decrease cell migration and invasion in HCC (12). In this study, we established SK-Hep-1 cell lines transfected with antisense oligonucleotide (ODN) of MZF-1. Characterization of these cells regarding the tumorigenicity *in vitro* and *in vivo* was performed. We found that inhibition of MZF-1 exerted inhibitory effects on the proliferation of SK-Hep-1 cells. Antisense ODN-mediated suppression of MZF-1 also inhibits tumor growth in human hepatocellular carcinoma xenografts in nude mice. Thus, MZF-1 may be controling the proliferative potential of HCC cells, acting as a tumorigenic factor in HCC.

Materials and Methods

Cell Culture

SK-Hep-1 cell line was purchased from the American Type Culture Collection (Rockville, MD, USA). The SK-Hep-1 cell line is poorly differentiated (1). The cell lines were cultured with DMEM (Gibco BRL) supplemented with 100 μM non-essential amino acid, 2 mM glutamate, 10% fetal bovine serum (FBS), 100 units/ml penicillin G, and 100 μg/ml streptomycin (Sigma Chemicals Co., St. Louis, MO, USA) in a humidified atmosphere containing 5% CO_2 at 37°C.

Antisense Knockout Assay

The antisense knockout assay was performed as described (20) and the following antisense and sense (as a control) sequences were used: MZF-1 (antisense ODN 5′-TACACAAGGGGACCATTCATTC-3′, AS-MZF-1; sense ODN 5′-GAATGAATGGTCCCCTTGTGTA-3′, S-MZF-1) (12). The cells were plated at 70% density 24 h before sense or antisense oligonucleotide treatment and then washed in triplicate with serum-free DMEM and incubated with sense or antisense oligonucleotide (0 μM, 1 μM, 2 μM, or 5 μM) in serum-free DMEM containing 10 μg/ml lipofectin (Life Technologies, Grand Island, NY, USA) at 37°C. The medium was changed to 10% FBS DMEM medium 6 h later before culturing at 37°C for 48 h.

RNA Isolation

The total RNA was isolated from cells by the guanidinium thiocyanate-phenol method (4). The HCC cell lines were homogenized (4 M guanidine thiocyanate, 25 mM sodium citrate, 0.5% (w/v) sodium laurylsarcosinate, 0.1 M β-mercaptoethanol) in a polypropylene tube. The total RNA was isolated using a standard method. Phenol/Chloroform reagent was added to the samples, and centrifuge the tube at 12,000 × g for 30 min at 4°C. RNA was precipitated from the aqueous phase using isopropanol, then the resultant pellet was washed twice with 70% ethanol. The RNA content of the resuspended pellet was quantified and checked for purity and condition by spectrophotometry at a wavelength of 260 nm. The extract integrity was assessed by 1.5% agarose gel electrophoresis and RNA was visualized by ethidium bromide staining.

Reverse Transcriptase (RT)-PCR

RT-PCR assay was done with slight modifications (6). An aliquot of total RNA (0.5 μg) was reverse by transcribed using 0.5 μM oligo d(T) primers in a reaction solution (50 μl) containing 75 mM KCl, 50 mM Tris-HCl (pH 8.3), 3 mM $MgCl_2$, 10 mM DTT, 10 U RNase inhibitor (Promega, Madison, WI, USA), 0.8 mM total dNTPs, and 200 units of moloney murine leukemia virus reverse transcriptase (Promega). The sample was incubated at 42°C for 1 h and at 99°C for 5 min before being chilled on ice for 10 min.

The RT product (2 μl) was diluted with the PCR buffer (50 mM KCl, 10 mM Tris-HCl, and 2 mM $MgCl_2$) to a final volume of 50 μl, containing 0.5 μM dNTPs (final concentration, 0.8 mM) and 0.5 unit of Super-Therm Taq DNA polymerase (Southern Cross Biotechnology, Cape Town, South Africa). PCR was performed on a GeneAmp PCR system 2400 (Applied Biosystems, Foster City, CA, USA). To avoid the PCR products to the plateau phase, in our preliminary data we have tested different amounts of RNA (0.1, 0.5, 1 and 2 μg) and differents cycle number (21, 23, 25, 27, 29, 31, 33 and 35 cycle). In each experiment, up to 33 cycles were performed to avoid reaching the PCR plateau values. The PCR products were analyzed by 1.5% agarose gel electrophoresis and direct visualization after SYBR Green I (Cambrex Bio Science Rockland, Inc., Rockland, ME, USA) staining. The agarose gels were scanned and analyzed using the Kodak Scientific 1D Imaging System (Eastman Kodak Company, New Haven, CT, USA). The relative mRNA density (Dm) was calculated using a formula: Dm = mRNA density/β_2-MG mRNA density. The β_2-MG is considered as internal control. The accuracy of the amplification reaction for each set of primers was determined by amplifying several dilutions of the same

cDNA with the same cycling profiles and amplifying the same cDNA dilution with different cycling profiles. The specificity of the cDNA was also checked using DNA sequence analysis (data not shown).

Oligonucleotide Synthesis

The primers used in RT-PCR were as follows: MZF-1, PKCα, PKCδ, PKCε, PKCι and β_2-MG as internal control and described previously (12).

Western Blotting

The cultured cells were washed twice with PBS and then lysed with a lysing buffer (50 mM Tris/HCl (pH 7.4), 2 mM EDTA, 2 mM EGTA, 150 mM NaCl, 1 mM PMSF, 10 μg/ml leupeptin, 10 μg/ml aprotinin, 10 μg/ml trypsin inhibitor, 1 mM NaF, 1 mM sodium orthovanadate, 1% (v/v) 2-mercaptoethanol, 1% (v/v) Nonidet P40, 0.3% sodium deoxycholate). The cell lysates were centrifuged at 100,000 × g and 4°C for 30 min. The supernatant was then collected and the protein concentration was then determined by the Bradford method. Each sample (40 μg) was then separated by SDS-PAGE using a 10% (w/v) gel and electrophoretically transferred onto a PVDF membrane (Millipore, Belford, MA, USA). The membrane was blocked with 5% (w/v) non-fat dried milk in TBST buffer (20 mM Tris, HCl (pH 7.4), 150 mM NaCl, 0.1% (v/v) Tween 20) and then incubated with the specific anti-MZF-1 (1:500) or α-tubulin (1:3000) antibody at 4°C overnight. After washing with TBST, the blots were then incubated with HRP-conjugated anti-mouse antibody (1:3000) at room temperature for 1 h and then washed with TBST before being visualized using chemiluminescence (Amersham Pharmacia Biotech, Piscataway, NJ, USA). The photographs of protein results were used to measure the level of density of MZF-1 protein bands by densitometry (Kodak Scientific 1D Imaging System; Eastman Kodak Company, New Haven, CT, USA). The relative protein density (Dp) was calculated using a formula: Dp=protein density/α-tubulin protein density. The α-tubulin is considered as internal control.

Cell Proliferation Assay

Cell proliferation was determined by the yellow tetrazolium MTT assay (22). To evaluate the effects of antisense ODN MZF-1 on the proliferation of SK-Hep-1 cell lines, 3-(4, 5-dimethylthiazol-2yl)-2, 5-diphenyl-2H tetrazolium bromide (MTT) assay was carried out. Briefly, 2×10^4 cells were seeded in 24-well microplates and cultured for 24 h. Then, antisense or sense ODN MZF-1 was added to the wells to the indicated concentrations. The cells were cultured for another 24 h and 48 h and the medium in each well was then replaced with 1 ml of fresh medium containing 5 mg/ml MTT. After an additional incubation for 4 h, the medium was discarded and 1 ml of isopropanol was added to each well to dissolve formazan crystals. Then, the optical density was read with an automated microplate reader at 570 nm. Cells at the log phase were used to calculate the doubling time according to the equation doubling time (h) = [log 2 × (24 × No. of days)]/[log densityfinal - log densityinitial]. Experiments were carried out in triplicate, and the results were shown as mean ± SD of three independent experiments.

Tumorigenicity Assay in Nude Mice

Female BALB/c nude mice, 4 ~ 6 weeks of age, were purchased from National Health Research Institute (Taipei, Taiwan, ROC), housed in a dedicated nude mouse facility with microisolator caging. The SK-Hep-1 cells were first treated with 5 μM antisense or sense ODN MZF-1, detached by trypsinisation 48 h later, and then washed in triplicate in serum-free DMEM. 1×10^7 cells in 100 μl volume was injected subcutaneously into the right posterior flank of mice by use of a 1 ml syringe with 24-gauge needle (23). The mice were randomly assigned to a treatment group: sense ODN MZF-1 (5 μM, 0.1 ml/mouse), S-MZF-1; antisense ODN MZF-1 (5 μM, 0.1 ml/mouse), AS-MZF-1. There were five mice in each group, and the experiment was repeated twice. The tumor volume was calculated by the formula: $0.5236 \times L1(L2)^2$, where L1 is long diameter, and L2 is short diameter (21). The inhibitory rate of tumor growth was calculated by the formula: (tumor $\text{volume}_{\text{S-MZF-1}}$-tumor $\text{volume}_{\text{AS-MZF-1}}$/ tumor $\text{volumeS}_{\text{-MZF-1}}$) × 100%.

Statistical Analysis

The data were expressed as mean ± standard deviations and were compared using Student's *t*-test.

Results

Effect of Antisense ODN MZF-1 on the MZF-1 mRNA and Protein Level

To verify the effects of antisense ODN in depleting the expression of MZF-1 mRNA and protein, we transfected the HCC cells with 0, 1, 2 and 5 μM sense or antisense ODN against MZF-1. MZF-1 mRNA and protein expression were analyzed by semiquantitative RT-PCR. MZF-1 mRNA was down-regulated according to the increase in antisense ODN concentration, although sense ODN did not show any effect on the MZF-1 mRNA (Fig. 1A, upper panel). The MZF-1 production at the dosage of 5 μM antisense ODN was suppressed

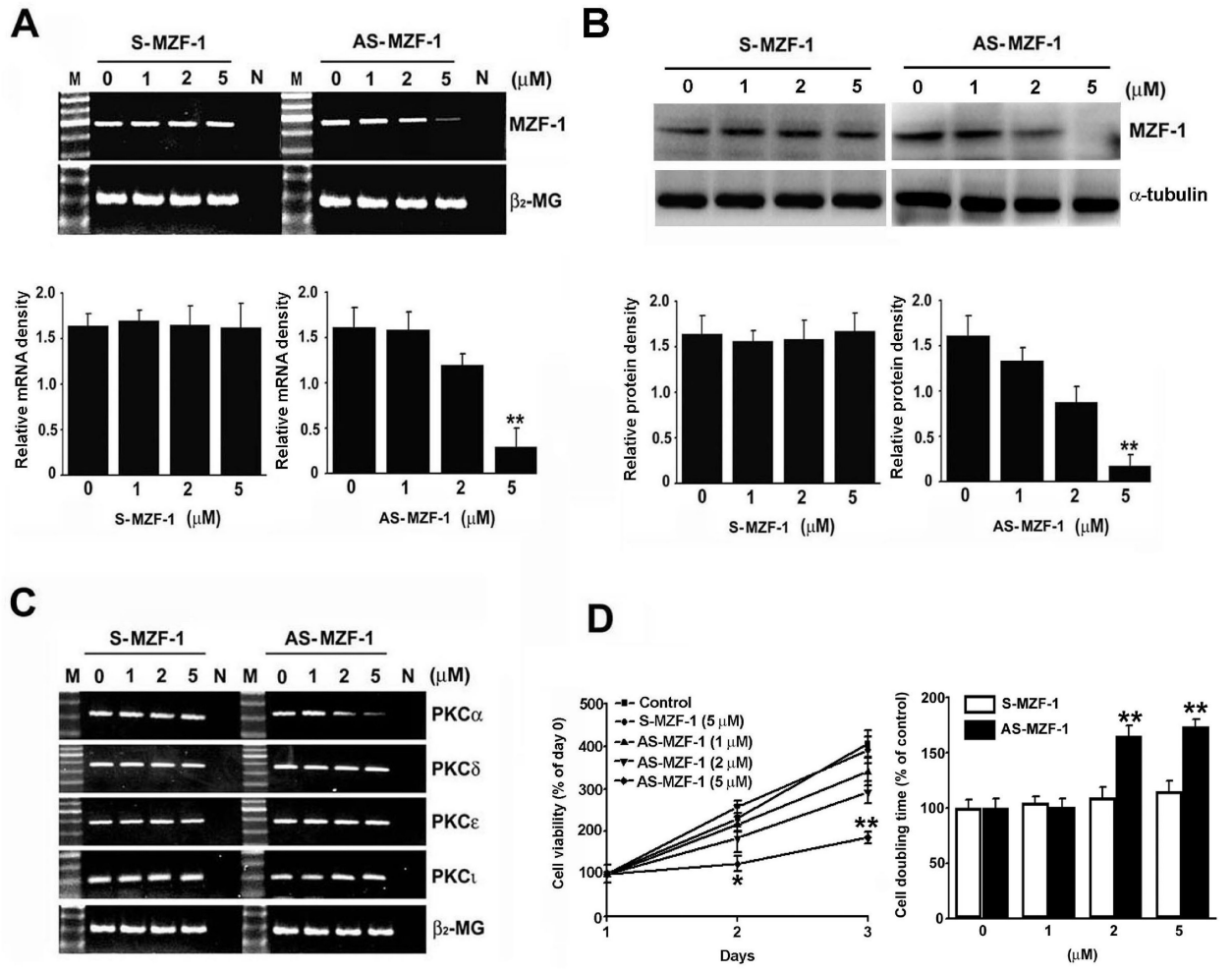

Fig. 1. Effect of antisense ODN MZF-1 on the mRNA and protein expressions and cell growth. (A) Effect of antisense ODN MZF-1 (AS-MZF-1) or sense ODN MZF-1 (S-MZF-1) on the levels of MZF-1 mRNA detected by semiquantitative RT-PCR in SK-Hep-1 cells on day 2 after treatment as described in Materials and Methods. The quantitative analysis of the semiquantitative RT-PCR was performed. (B) Effect of antisense ODN on the levels of MZF-1 protein detected by western blotting in SK-Hep-1 cells on day 2 after treatment as described in Materials and Methods. The quantitative analysis of the western blotting was performed. The data represent one of three independent experiments with similar results. $^{**}P < 0.01$ *versus* control. (C) Effect of antisense ODN MZF-1 on the levels of PKC isoforms mRNA detected by semiquantitative RT-PCR in SK-Hep-1 cells on day 2 after treatment as described in Materials and Methods. The data represent one of three independent experiments with similar results. (D) Effect of antisense ODN MZF-1 on cell viability (left panel) and cell doubling time (right panel). The SK-Hep-1 cells were transfected with either the indicated μM MZF-1 antisense ODN or 5 μM sense ODN. Cell growth was determined using the MTT assay as described in Materials and Methods. Control, the group was treated with 0 μM MZF-1 antisense ODN. Data are presented as means ± SE of 3 replicates from 2 independent experiments. $^{*}P < 0.05$ *versus* control; $^{**}P < 0.01$ *versus* control.

to 15% in control cultures of 0 M dosage (Fig. 1A, lower panel). These altered patterns of the mRNA expressions were consistent with the protein expression levels determined using Western blotting (Fig. 1B).

Effect of Antisense ODN MZF-1 on the mRNA Levels of PKC Isoforms

To confirm that MZF-1 is involved in the expression of PKCα mRNA in SK-Hep-1 cells, the mRNA expressions of PKC isoforms were analyzed by semi-quantitative RT-PCR. PKCα mRNA was down-regulated in SK-Hep-1 cells treated with antisense ODN MZF-1, but it was not down-regulated in SK-Hep-1 cells treated with sense ODN (Fig. 1C). PKCα preotein level at the dosage of 5 μM antisense ODN was suppressed to 30% in control cultures of 0 M dosage, whereas the antisense ODN MZF-1 made no effect on the other PKC isoforms.

Effect of Antisense ODN MZF-1 on Cell Proliferation

It has been demonstrated that antisense ODN

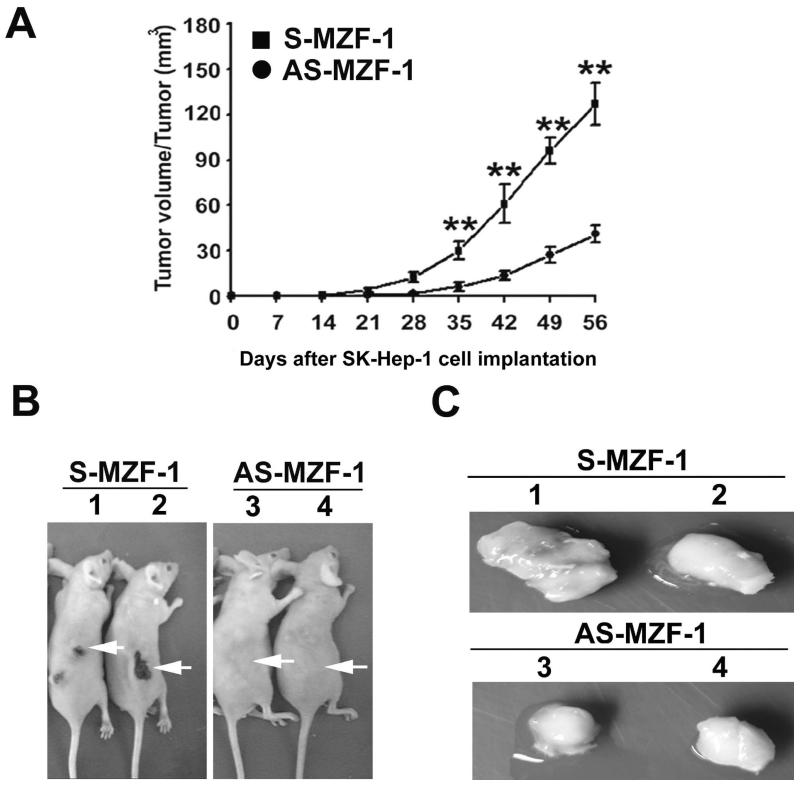

Fig. 2. Suppression of tumorigenesis in antisense ODN-transfected cells. (A) Tumor growth curve in S-MZF-1 (5 μM; ●) or AS-MZF-1 (5 μM; ■) transfected human SK-Hep-1 xenografts (n = 5). A total of 5×10^6 sense or antisense ODN MZF-1 pretreated cells were injected into the flank region of nude mice. Tumor development was followed up to 2 months, and mice then were sacrificed. Cross sectional tumor diameters were measured externally, and the approximate tumor volume was calculated as described in Materials and Methods. The results represent the mean ± SD of five developed tumors in the experimental mice. $^{**}P < 0.01$ *versus* S-MZF-1 pretreated group. (B) The visible tumor formed by the indicated pretreated cells on day 56. (C) Photographs of the representative tumors removed from mice on day 56.

MZF-1 specifically inhibited MZF-1 mRNA expression, resulting in lower levels of MZF-1-within treated tumor cells. To determine whether such antisense ODN MZF-1 mediated inhibition of MZF-1 resulted in changes in cell proliferation, the effects of such treatment on *in vitro* tumor cell growth were examined. Antisense ODN MZF-1 showed a dose-dependent reduction in cell proliferation (Fig. 1D, left panel), and cell doubling time increased from 101.2% of the control for 1 μM antisense ODN to 165.5% for 2 μM antisense ODN (Fig. 1D, right panel). Moreover, cell proliferation was completely inhibited by 5 μM antisense ODN and the doubling time was 173.4% of the control.

Effect of Antisense ODN MZF-1 on the Tumorigenicity of SK-Hep-1 Cells

Because antisense ODN MZF-1 specifically inhibited MZF-1 expression and inhibited cell growth, we then further examined the effects of antisense ODN MZF-1 on tumor formation. The experiment was performed by injecting 5×10^6 sense or antisense ODN MZF-1 pretreated SK-Hep-1 cells into nude mice and monitored the mice for tumor morphological observation and growth. The sense ODN MZF-1-pretreated cells displayed rapid formation and growth of tumors (Fig. 2, A, B and C), like the untreated-control cells (data not shown). In contrast, the mice injected with antisense ODN MZF-1-pretreated cells developed slow-growing tumors. The maximum inhibitory rate of tumor growth was 74.2 ± 4.6% (n = 5) and the mean of inhibitory rate of tumor growth from 28 days to 56 days was 71.2 ± 8.6 %. The tumor formation time was prolonged from 14 days to 26 days, since it showed significant difference ($P < 0.01$) between the antisense-treated group (26.3 ± 6.6 days) and the sense-treated group (14.2 ± 2.7 days).

Discussion

In this study, we used antisense ODN technique to specifically knock-out MZF-1 expression in HCC cells and found that the antisense ODN MZF-1 also has efficient and specific down-regulation of MZF-1 mRNA and protein, as previously by shown (12),

which is a significant reduction of PKCα mRNA and protein expression. Significantly, antisense ODN MZF-1-mediated knock-out expression of MZF-1, inhibited cellular proliferation and tumor formation in nude mice. These studies suggested a novel role of MZF-1 in the regulation of tumorigenesis in HCC cells.

Recent data obtained from knockout mice have begun to provide *in vivo* evidence of the role of MZF-1, including the role of MZF-1 in tumorigenesis. Gaboil *et al*. report that mice lacking MZF-1 show increased tumorigenesis. Hence, MZF-1 is suggested to act as a tumor suppressor in tumorigenesis (8). In contrast, some studies have found that over-expression of MZF-l aggressively transforms NIH3T3 cells. These transformed NIH3T3 cells traverse the cell cycle more rapidly, form foci, form colonies in soft agar, and form tumors in nude mice (10). The retrovially overexpressing MZF-1 in IL-3-dependent FDCP.1 cells inhibited their apoptosis when IL-3 was withdrawn (11). The MZF-1-transduced FDCP.1 cells also formed tumors when injected into congenic mice. From these points of view, MZF-1 has bifunctional transcriptional regulatory properties depending on the cellular environment. However, our data agreed with the later experiments that MZF-1 may be involved in the tumorigenesis of human HCC cells.

The antisense strategies have been used in a variety of eukaryotic systems both to understand normal gene function and to block gene expression therapeutically *in vitro* (2). In this study, we demonstrated that human HCC cells can be successfully treated by liposome-mediated antisense ODN MZF-1. In addition, the incomplete delivery of the antisense ODN MZF-1 might be responsible for the lack of a complete anticancer effect. Thus, although we showed tumor inhibition, we did not observe tumor regression. One explanation is that nontransfected cells can still release MZF-1 and induce tumorigenesis. In the future, transfecting liposome/vector complexes and multiple injection of the complex into the tumor may be necessary to improve the delivery of the antisense molecules and either induce tumor regression or inhibit tumor growth for a long period of time. However, our data show the *in vitro* and *in vivo* anti-tumorigenesis effect of antisense ODN MZF-1.

Acknowlegments

We thank Dr. Jaw-Ji Yang for valuable comments and suggestions. This work was supported by a grant from the National Science Council, Taiwan, Republic of China (NSC 94-2320-B-040-016).

References

1. Aden, D.P., Fogel, A. and Plotkin, S. Controlled synthesis of HBsAg in a differentiated human liver carcinoma-derived cell line. *Nature* 282: 615-616, 1979.
2. Agrawal, S. Antisense oligonucleotides as antiviral agents. *Trends Biotechnol*. 10: 152-158, 1992.
3. Bavisotto, L., Kaushansky, K., Lin, N. and Hromas, R. Antisense oligonucleotides from the stage-specific myeloid zinc finger gene MZF-1 inhibit granulopoiesis *in vitro*. *J. Exp. Me*d. 174: 1097-1101, 1991.
4. Chomczynski, P. and Sacchi, N. Single-step method of RNA isolation by acid guanidinium thiocyanate-phenol-chloroform extraction. *Anal. Biochem*. 162: 156-159, 1987.
5. Cox, P.M. and Goding, C.R. Transcription and cancer. *Brit. J. Cancer* 63: 651-662, 1991.
6. De Petro, G., Tavian, D., Copeta, A., Portolani, N., Giulini, SM. and Barlati, S. Expression of urokinase-type plasminogen activator (u-PA), u-PA receptor, and tissue-type PA messenger RNAs in human hepatocellular carcinoma. *Cancer Res*. 58: 2234-2239, 1998.
7. Dunaeva, M., Michelson, P., Kogerman, P. and Toftgard, R. Characterization of the physical interaction of Gli proteins with SUFU proteins. *J. Biol. Chem*. 278: 5116-5122, 2003.
8. Gaboli, M., Kotsi, P.A., Gurrieri, C., Cattoretti, G., Ronchetti, S., Cordon-Cardo, C., Broxmeyer, H.E., Hromas, R. and Pandolfi, P. P. Mzf1 controls cell proliferation and tumorigenesis. *Genes Dev.* 15: 1625-1630, 2001.
9. Hromas, R., Collins, S.J., Hickstein, D., Raskind, W., Deaven, L.L., O'Hara, P., Hagen, F.S. and Kaushansky, K. A retinoic acid responsive human zinc finger gene, MZF-1, preferentially expressed in myeloid cells. *J. Biol. Chem*. 266: 14183-14187, 1991.
10. Hromas, R., Morris, J., Cornetta, K., Berebitsky, D., Davidson, A., Sha, M., Sledge, G. and Rauscher, F 3rd. Aberrant expression of the myeloid zinc finger gene, MZF-1, is oncogenic. *Cancer Res.* 55: 3610-3614, 1995.
11. Hromas, R., Boswell, S., Shen, R.N., Burgess, G., Davidson, A., Cornetta, K., Sutton, J. and Robertson, K. Forced over-expression of the myeloid zinc finger gene MZF-1 inhibits apoptosis and promotes oncogenesis in interleukin-3-dependent FDCP.1 cells. *Leukemia* 10: 1049-1050, 1996.
12. Hsieh, Y.H., Wu, T.T., Tsai, J.H., Huang, C.Y., Hsieh, Y.S. and Liu, J.Y. PKC alpha expression regulated by Elk-1 and MZF-1 in human HCC cells. *Biochem. Biophys. Res. Commun*. 339: 217-225, 2006.
13. Ladomery, M. and Dellaire, G. Multifunctional zinc finger proteins in development and disease. *Ann. Hum. Genet.* 66: 331- 342, 2002.
14. Liu, P., Keller, J.R., Ortiz, M., Tessarollo, L., Rachel, R.A., Nakamura, T., Jenkins, N.A. and Copeland, N.G. Bcl11a is essential for normal lymphoid development. *Natl. Immunol.* 4: 525-532, 2003.
15. Moms, J., Hromas, R. and Rauscher, F.111. Characterization of the DNA binding properties of the myeloid zinc finger gene MZF-1: Two independent DNA-binding domains recognize two DNA consensus sequences with a common G-rich core. *Mol. Cell. Biol.* 14: 1786-1795, 1994.
16. Morris, J.F., Rauscher, F.J., Davis, B., Klemsz, M., Xu, D., Tenen, D. and Hromas, R. The myeloid zinc finger gene, MZF-1, regulates the CD34 promoter *in vitro*. *Blood* 86: 3640-3647, 1995.
17. Murai, K., Murakami, H. and Nagata, S. Myeloid-specific transcriptional activation by murine myeloid zinc-finger protein 2. P*roc. Natl. Acad. Sci. USA* 95: 3461-3466, 1998.
18. Papavassiliou, A.G. Transcription factors: structure, function, and implication in malignant growth. *Anticancer Res.* 15: 891-894, 1995.
19. Robertson, K.A., Hill, D.P., Kelley, M.R., Tritt, R., Crum, B., Van, Epps. S., Srour, E., Rice, S. and Hromas, R. The myeloid zinc finger gene (MZF-1) delays retinoic acid-induced apoptosis and differentiation in myeloid leukemia cells. *Leukemia* 12: 690-698, 1998.
20. Shen, L., Dean, N.M. and Glazer, R.I. Induction of p53-dependent, insulin-like growth factor-binding protein-3-mediated apoptosis in glioblastoma multiforme cells by a protein kinase Calpha antisense

oligonucleotide. *Mol. Pharmacol*. 55: 396-402, 1999.
21. Singh, R.P., Dhanalakshmi, S., Tyagi, A.K., Chan, D.C., Agarwal, C. and Agarwal, R. Dietary feeding of silibinin inhibits advance human prostate carcinoma growth in athymic nude mice and increases plasma insulin-like growth factor-binding protein-3 levels. *Cancer Res*. 62: 3063-3069, 2002.
22. Sobottka, S.B. and Berger, M.R. Assessment of antineoplastic agents by MTT assay: partial underestimation of antiproliferative properties. *Cancer Chemother. Pharmacol*. 30: 385-393, 1992.
23. Takei, Y., Kadomatsu, K., Matsuo, S., Itoh, H., Nakazawa, K., Kubota, S. and Muramatsu, T. Antisense oligodeoxynucleotide targeted to midkine, a heparin-binding growth factor, suppresses tumorigenicity of mouse rectal carcinoma cells. *Cancer Res.* 61: 8486-8491, 2001.